



Project: **SEAWave**

## **DNA methylation pattern in combination with/analysis of differentially expressed genes**

Work Package: WP8

Deliverable: D8.2

Deliverable No.: D28

## Abstract

In work package 8, we investigated whether fifth generation of mobile telephony frequency range 2 (5G FR2) has effects on oxidative DNA stress, transcriptomics and epigenetics on primary skin cells. After carefully selecting the primary epidermal adult and juvenile keratinocytes and adult melanocytes, we exposed the cells to FR2 millimeter waves at 27.5 GHz with different power densities (10 W/m<sup>2</sup>, 3.33 W/m<sup>2</sup>, and sham exposure). 5G FR2 did not induce any oxidative DNA stress in all tested cells and caused no gene expression changes in adult melanocytes and keratinocytes. However, 5G FR2 was predicted to inhibit and activate some pathways in juvenile keratinocytes. The DNA methylation assay is as of 25.06.2025 ongoing and estimated to be finished on 15.07.2025.

## Project Details

Project name	SEAWave
Grant number	101057622
Start Date	01 Jun 2022
Duration	42 months
Scientific coordinator	Prof. Th. Samaras, Aristotle University of Thessaloniki (AUTH)

## Deliverable Details

Deliverable related number	D8.2
Deliverable No.	D28
Deliverable name	DNA methylation pattern in combination with/analysis of differentially expressed genes
Work Package number	WP8
Work Package name	Health Risk Studies: Biological Effects of FR2 Exposure on Human-derived Skin Cells
Editors	Dr. A. Bitsch, M. Djuari, Dr. C. Ziemann, ITEM
Distribution	Public
Version	1
Draft/final	Final
Keywords	DNA methylation, transcriptomics, epigenetics

## Table of Contents

1	Introduction .....	4
2	Skin cell model selection.....	5
3	Assays.....	8
3.1	Genotoxicity and oxidative DNA stress.....	8
3.2	Transcriptomics.....	9
3.3	Epigenomics .....	10
4	Methods.....	11
4.1	Cell culture .....	11
4.2	Cell exposure to 5G FR2 .....	11
4.3	hOGG1-modified <i>in vitro</i> alkaline comet assay .....	12
4.4	Transcriptome analysis .....	13
4.5	DNA methylation.....	14
5	Results.....	15
5.1	hOGG1-modified <i>in vitro</i> alkaline comet assay .....	15
5.2	Transcriptomics.....	17
5.3	DNA methylation assay.....	22
6	Conclusions .....	23
7	References .....	24

## 1 Introduction

In work package (WP) 8 of SEAWave project, we are investigating the biological effects of fifth generation of mobile telephony (5G) in frequency range 2 (FR2), millimeter waves in *in vitro* settings. One of the main foci in this WP is to examine the carcinogenic potential of 5G FR2 exposure and thus to estimate potential adversity of electromagnetic fields (EMF) on human health.

In the present WP part, and main objective of D8.2, ITEM focused on early changes in the epigenetic and transcriptomic landscapes of skin cells *in vitro* after short term exposure to 5G FR2. Both endpoints are related to deregulation of gene expression at different levels. Epigenetic events comprise amongst others DNA methylation and histone variants as known modulators of gene expression. In general, epigenetic processes are inherent parts of normal development, but abnormal changes in the epigenome can lead to the development of diseases, including cancer. These effects often result from exposure to environmental factors such as diet, smoke, but also radiation and probably EMF. Indeed, several studies could demonstrate epigenetic modifications induced by ionizing radiation [1]. Extremely low frequency magnetic fields (ELF-MF) might stabilize active chromatin, particularly during the transition to an active state during cell differentiation [2]. In the ARIMMORA project, ELF-MF were investigated in a mouse model to determine potential disruptions in the genome, transcriptome and epigenome, leading to childhood leukemia. The evaluated genes included, amongst others, the cell adhesion molecule 1 (Cadm1), a tumor suppressor gene frequently inactivated in human cancer by promoter hypermethylation; overall a higher percentage of methylation in spleen tissues of mice exposed to 50 Hz 10 mT ELF-MF was detected [3].

Transcriptomic fingerprints derived from tumor-specifically deregulated genes are known for certain types of tumors. As the skin is a directly radiation-exposed tissue, also including EMF, potential induction of inflammation or even tumor development is worth to consider as potential adverse effect of EMF. One of the most dangerous types of skin cancer are melanomas, which develop from pigment-producing melanocytes. Melanomas are highly metastasis-forming tumors, and thus, probably the most critical skin cancer type for humans. They typically occur in the skin but may also rarely occur in the mouth, intestines or eye (uveal melanoma). About 25% of melanomas develop from a type of chronic lesion, i.e., induced by UV light. Comprehensive gene expression profiling identified upregulation of activators of cell cycle progression, DNA replication, and repair as important events in melanoma development [4] as well as modification of the DNA methylation landscape [5]. Further changes included upregulation of genes associated with resistance to apoptosis and loss of genes associated with cellular adhesion and melanocyte differentiation.

Up until now, there are only a few publications, which examined the biological effects of 5G FR2 on the skin but mostly focused on skin pigmentation [6-9]. There is one recent study, which investigated the effects of 5G FR2 exposure on gene expression and DNA methylation changes

using spontaneously transformed aneuploid immortal keratinocytes cell line from adult human skin HaCaT [10]. However, the effects of 5G FR2 exposure in primary skin cells are still largely unknown. Therefore, we conducted experiments to detect exposure-related changes in gene expression (transcriptomics) and DNA methylation (epigenetics) in primary human-derived skin cells to identify early markers and mode of action for potential 5G FR2 induced tumorigenesis. As reported in D8.1, we received the exposure system and performed respective acceptance tests in March 2024. The exposure system functions in a blinded manner by randomly selecting the exposure condition for every exposure chamber with no knowledge by the experimenter. Cells are exposed in 25 cm<sup>2</sup> flasks to FR2 millimeter waves at 27.5 GHz with 100 MHz bandwidth in 3 different power density (10 W/m<sup>2</sup>, 3.33 W/m<sup>2</sup> and sham exposure).

After careful selection and characterization of primary human-derived skin cells as model systems, cells were exposed to the 5G FR2 for 24 h with 10 min on and 5 min off. Then we harvested the cells, isolated RNA and DNA, and processed the samples further using array technologies to be able to detect both changes in gene expression and DNA methylation, which might indicate a carcinogenic potential of 5G FR2.

## 2 Skin cell model selection

The first step in work package 8 was to choose appropriate human skin cell models. As pre-requisites, the skin cell models should cover as many population doublings as possible and have little preexisting damage to avoid any artifacts in 5G FR2 testing. Finally, primary human keratinocytes and melanocytes were selected as model systems, because these cells are the main cell types of the epidermis in human skin (see Figure 1). Light-pigmented donors were preferred, due to better availability from European providers and therefore also representing the dominant skin type with Europe. Cells from single donors were preferred for a more accurate comparison of replicates in gene expression analyses.

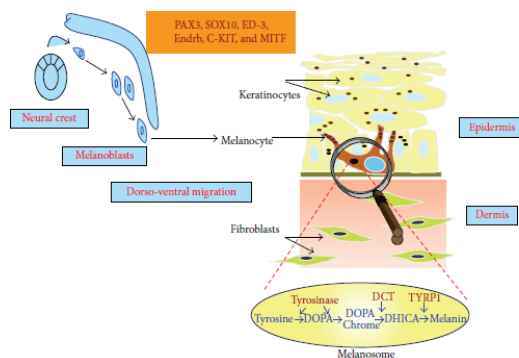


Figure 1: Overview of structural component of human skin [11].

The tissue origin was also an important point to be considered during cell model selection. To be able to simulate the real-life situation, tissue from the facial area was preferred, as, normally,

mobile phone usage occurs in the near facial area of the body, i.e. during phone calls, and selected the eyelid as cell source, because this body part is mostly protected from UV rays during the day. Additionally, this is one of the few body parts to have normal skin excised due to age-related loss of underlying dermis' elasticity. Another important point is that the epidermis from eyelid is mostly physiologically and histologically normal [12, 13].

Finally, we choose PromoCell (Heidelberg, Germany) as cell provider, as PromoCell harbors the most comprehensive spectrum of skin cells, including availability of primary skin cells from adult donors.

To broaden the model cell population, we also planned to use primary keratinocytes from younger donors. At the time of inquiry, keratinocytes from the facial area of younger donors were not available. Therefore, we selected keratinocytes from a juvenile male donor, aged 1 year, isolated from foreskin. Foreskin is also one of the few body parts to have normal skin excised in younger males for religious reasons. Thus, the epidermis is also physiologically and histologically normal. Preexisting damage due to UV rays is also less of prevalence [14].

The consideration of using keratinocytes from both adult and juvenile donors is to consider age-related differences in gene expression. Adult skin had higher gene expression for some pathways, for example epidermal homeostasis, antigen processing, and hair cycle than younger skin. In contrast, younger skin had higher gene expression for extracellular matrix development and fatty acid metabolism than adult skin, which shows that the infant epidermal barrier is still under development [15].

We finally selected three primary human skin cell models for this WP part, i.e., normal human epidermal keratinocytes from both a juvenile and an adult donor (NHEK-f.c., male donor; NHEK-c., female donor, respectively) and normal human epidermal melanocytes from an adult donor (NHEM, female donor). An overview of each cell model is presented in table 1.

Table 1: Overview of selected primary skin cells ( PromoCell).

Name	Cell type	Sex	Age	Tissue origin	Ethnicity	Passage
<b>NHEK-f.c.</b>	Keratinocytes	male	1	foreskin	Caucasian	2
<b>NHEK-c.</b>	Keratinocytes	female	51	eyelid	Caucasian	2
<b>NHEM</b>	Melanocytes	female	56	eyelid	Caucasian	2

NHEK: normal human epidermal keratinocytes; NHEM: normal human epidermal melanocytes

All cells were characterized before being exposed to 5G FR2 in terms of population doubling time (PDT, information needed for the micronucleus assay), chromosome number (to evaluate correct cell identity), sensitivity in cytotoxicity assay and sensitivity to known chemical positive controls that might be used in the different assays.

NHEK-f.c. and NHEK-c. exhibited typical polygonal-shaped keratinocyte morphology (see Figure 2, right picture) and PDTs of 23.4 and 24.6 h, respectively, which were slightly slower than the

PDTs given by the supplier (18.3 and 22.6 h, respectively). NHEM displayed typical dendritic-shaped morphology with long, branching processes (see Figure 2, left picture) but had a significantly slower PDT of 80 h, compared to the given PDT of 48 h.

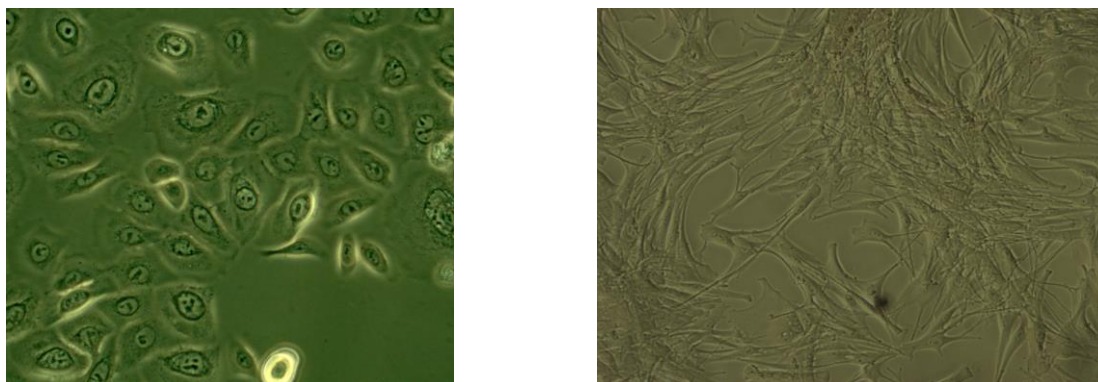


Figure 2: Morphology of primary juvenile human epidermal keratinocytes (NHEK-f.c., right) at passage 3, and freshly thawed primary adult human epidermal melanocytes (NHEM, left).

Additionally, we selected two melanoma cell lines to aid in the analysis of gene expression changes and DNA methylation. These cells served as a comparison to the exposed cells in terms of first signs of carcinogenesis in gene expression and DNA methylation. Human cell line MelHO, which was established from a primary tumor of a woman with melanoma in 1976, who carries the BRAF V600E mutation, but no NRAS Q61 mutation [16]. On the other hand, the human cell line IPC-298, established from a primary tumor of 64-year-old woman with cutaneous melanoma, was chosen, because it harbors the NRAS Q61L mutation, but no BRAF V600 mutation [17]. Both mutations play an important role in melanoma genesis [18].

MelHO and IPC-298 cells exhibited typical morphology, as described by the Leibniz Institute DSMZ-German Collection of Microorganisms and Cell Cultures GmbH (Braunschweig, Germany), which consists of epithelial-like cells with long, narrow shapes for MelHO and spindle-like cells for IPC-298 (see Figure 3). PDT of the cell lines amounted to 28.3 and 26 h, respectively.

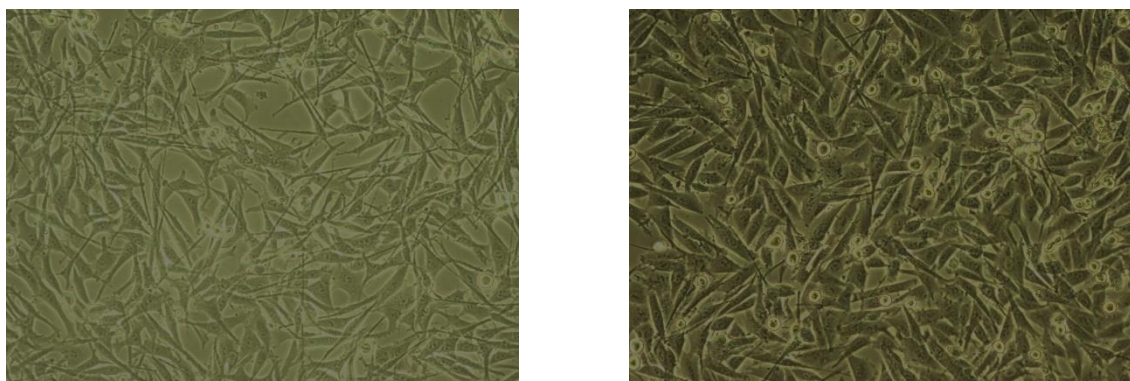


Figure 3: Morphology of cell lines MelHO (left) and IPC-298 (right) at passage 14 and 16, respectively.



### 3 Assays

#### 3.1 Genotoxicity and oxidative DNA stress

As oxidative stress and subsequent genotoxicity have been discussed as potential consequences of 5G FR2 exposure, these endpoints were investigated in pre-experiments to be able to anticipate related changes in the following gene expression analyses.

Genotoxicity is the ability of chemical or physical disruptors to induce DNA-base modifications, such as DNA adducts or DNA-strand breaks. This term is often confused with mutagenicity, which refers to the induction of permanent transmissible changes in the amount or structure of genetic material or organism. While all mutagens are genotoxic, not all genotoxin are mutagenic. Cells can prevent mutations from genotoxic events by complex DNA repair mechanisms or by induction of apoptosis (programmed cell death). Unrepaired DNA damage can finally lead to mutagenesis. Thus, in the case of induction of genotoxicity by 5G FR2, including oxidative DNA damage, DNA repair enzymes and antioxidative enzymes would represent interesting target genes for both gene expression changes and epigenetic modification.

One assay that can detect the DNA strand breaks in mammalian cells is *in vitro* alkaline comet assay. In this assay, exposed single cells are embedded in agarose sandwich on a microscope slide. The cell membrane is then lysed by exposing the DNA to alkaline pH <10, using a lysis buffer which contains, amongst others a detergent, such as Triton X-100. To be able to detect besides DNA double strand breaks also DNA single strand breaks, the exposed DNA is subjected to an unwinding step in electrophoresis buffer with a pH value of >13, and then electrophoresis is performed to enable migration of DNA fragments to the anode, resulting in a cometlike structure with head (undamaged DNA) and tail (DNA fragments). The slides are then neutralized and stained. Finally, the quantification of the DNA fragments in the comet tail is done using an image analyzing system, where tail intensity (TI, % DNA in tail) is measured (see figure 9).

This assay can be modified to also assess oxidative DNA damage by adding an enzyme incubation step with the DNA repair enzyme, i.e., human 8-oxoguanine glycosylase (hOGG1) after cell lysis and before electrophoresis (see Figure 9, number 4). This enzyme excises specifically the DNA adduct 8-oxoguanine (8-OHdG), which is a mutagenic base byproduct, resulting from DNA exposure to reactive oxygen species (ROS). By excising 8-OHdG DNA strand breaks arise, which allow quantification of oxidative DNA lesions in the comet assay.



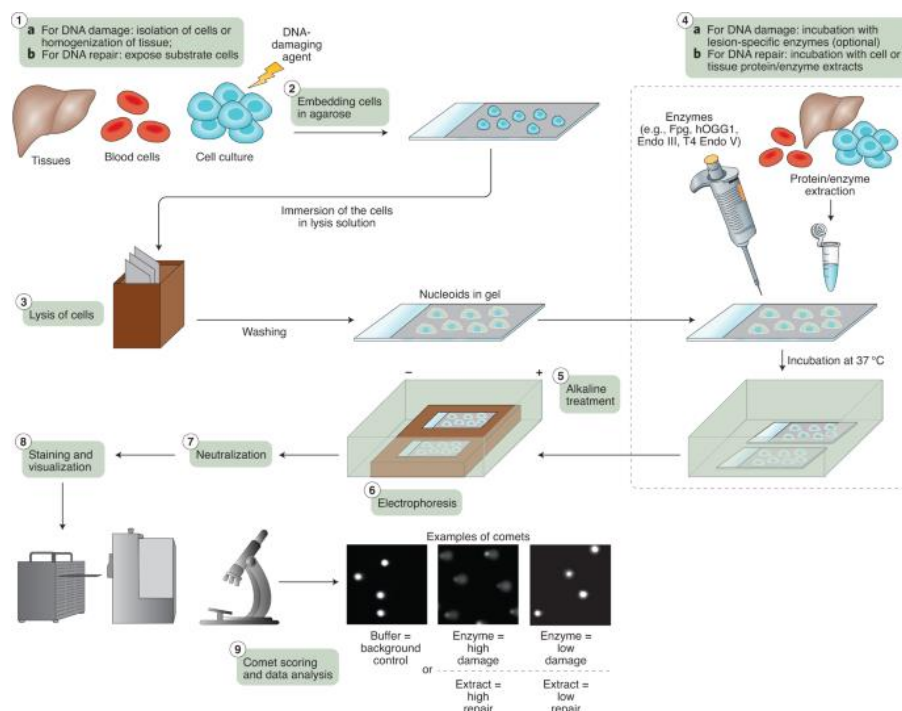


Figure 4: Scheme of comet assay procedure [19].

### 3.2 Transcriptomics

The term “transcriptomics” reflects the experimental evaluation of the transcriptome, and thus the whole set of RNA transcripts and their expression levels in cells at a given time. RNA serves diverse functions in a cell, such as transient intermediary molecule in the information network (mRNA) from gene to protein, but there are also additional regulatory functions from noncoding RNA. Due to these functions, transcriptomics can identify in a very sensitive way, specific stress responses of cells at a very early stage after an insult by measuring gene expressions. Transcriptomics can also be utilized to detect specific stress mechanism, because sets of induced genes trigger specific pathways [20].

In this project, we investigated genome-wide transcriptome changes after exposure to 5G FR2 using an Affymetrix microarray system, which is not only cost effective, but also can screen >20,000 well-annotated genes in short time. For this, total RNA was isolated from 5G FR2-exposed cells, followed by reverse transcription of the isolated RNA. Using the cDNA from the reverse transcription, the microarray was hybridized, and fluorescence signals were scanned (see Figure 5) [21].

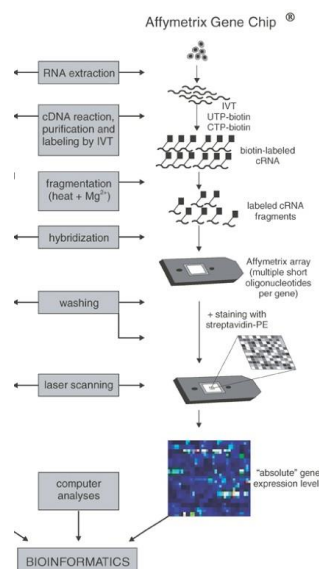


Figure 5: Overview of Affymetrix microarray system modified from Staal et al. [21].

After microarray scanning, the resulting gene expression data were analyzed regarding data quality, normalization, and differentially expressed genes (DEGs). Additionally, pathway and gene ontology enrichment analyses were performed to examine affected pathways.

### 3.3 Epigenomics

The transformation of normal cells into malignant ones is influenced by both genetic and epigenetic alterations. One of the epigenetic alterations is DNA methylation. In mammalian cells, DNA methylation primarily takes place as an addition of a methyl group to the cytosine of a cytosine-guanine dinucleotide (known as CpGs). So-called CpG islands in gene promoter regions are aberrantly methylated in cancer [22-24].

In this project, we screen epigenome-wide DNA methylation profiles using Illumina methylation array technology, which can target ~930,000 unique methylation sites. This method offers extensive coverage of CpG islands, genes, and enhancers. For this screening, we isolated DNA from cells after exposure to 5G FR2. After DNA quantification to ensure sufficient amount of DNA for the array, the isolated DNA undergoes bisulfite conversion to convert unmethylated cytosines to uracil. The samples are amplified, fragmented and precipitated, before hybridizing the samples to the array. After washing and staining of the array, the fluorescence signals are scanned [25].

Afterwards, the resulting data are analyzed in terms of data quality and differentially methylated genes (DMGs). Subsequently, pathway analyses are performed to predict affected pathways.

## 4 Methods

### 4.1 Cell culture

The original vials of the keratinocytes and melanocytes from PromoCell, Heidelberg, Germany were immersed in a 37 °C water bath until the cells detached from the vial wall. Immediately afterwards, the thawed cells were poured into pre-warmed Keratinocytes Growth Medium 3 or Melanocyte Growth Medium M3 (PromoCell) in a T75 cell culture flask and the vial was washed once with the cell suspension. The cells were then incubated for 24 h in a 37 °C/5% CO<sub>2</sub>, 95% H<sub>2</sub>O incubator. Thereafter, the medium was replaced with fresh medium to remove remaining freezing medium and incubated for few days until 90% confluence was reached.

To prepare the working cell batch for 5G FR2 exposure, the cells were then washed twice with 4 ml of pre-warmed phosphate buffer saline (PBS) and trypsinized using 0.05 % trypsin/ 0.02 % EDTA solution for 5 min at 37 °C. Afterwards, trypsin inhibitor and growth medium were pipetted into the cell suspension to quench trypsin activity. The cell suspension was transferred into a centrifuge tube and centrifuged at 303 x g for 5 min. After removing the supernatant, the cells were then resuspended in fresh pre-warmed CryoSFM freezing medium (PromoCell) in the needed cell density, followed by transfer of the cell suspension into cryovials and subsequently frozen using a Planer Kryo 10 Series II freezing device (Planer, Sunbury on Thames, United Kingdom) The cell working batch was then stored in the gas phase of nitrogen tank.

A week prior to 5G FR2 exposure, a vial from the working batch was thawed and incubated using the method described above. The cells were then pre-incubated for 72 h (NHEK) or 96 h (NHEM) in a 37 °C/5% CO<sub>2</sub>, 95% H<sub>2</sub>O incubator prior to cell plating before FR2 exposure.

### 4.2 Cell exposure to 5G FR2

The cells were exposed to 5G FR2 at 27.5 GHz with 100 MHz bandwidth using the exposure system developed by IT'IS Foundation (Zürich, Switzerland). The system comprises a computer-controlled system rack with radiofrequency (RF) source, power supplies, and data acquisition, as well as three shielded chambers to operate in three different power densities of 10 W/m<sup>2</sup> (high power density or high), 3.33 W/m<sup>2</sup> [low power density (low)] and sham (no 5G RF2) exposure.

The built-in sensors monitor and record the exposure conditions and control exposure, such as temperature and fan current for airflow needed for the cell cultures. Each shielded chamber can contain four T25 flasks inserted directly into an internal support structure.

A pre-check of this exposure system included the measurement of heat development and the effect on survival and growth of cells in culture.

At 24 (NHEK) or 72 h (NHEM) prior to 5G FR2 exposure, the cells were trypsinized using the method described under 4.1 with the modification of resuspension of cell pellets in a growth

medium. The cells were then plated in at minimum three T25 cell culture flask with cell densities between  $0.375 \cdot 10^6$  and  $10^6$  cells/flask, depending on the assay type. On the day of exposure, the medium in the cell culture flask was replaced with 8 ml of growth medium.

The cells were then inserted into the exposure chambers. If there were < four flasks with cells to be exposed in each chamber, additional T25 cell culture flasks filled with 8 ml cell culture medium were added to the empty slots to ensure accurate exposure to 5G FR2. Afterwards, the exposure settings were inputted in the controller software and the exposure was started with 30 min delay to ensure temperature stabilization in the incubator harboring the exposure units. The cells were exposed in a blinded manner, where the power density of each chamber is selected randomly by the computer and hidden during exposure. Decoding of the blinded experiments was done by IT'IS Foundation after finishing assay analysis.

The exposure duration was chosen based on available publications on *in vitro* studies. Since there were only a few studies available, investigating biological effects of 5G FR2, we also included *in vitro* publications which examined exposure to frequency range 1 (FR1) microwave. In total 380 *in vitro* publications were found during the search in literature databases, such as EMF Portal, PubMed, Scopus and ScienceDirect. After excluding studies with inadequate exposure setup and reviews, 164 publications were selected for further analyses. In these publications, in total of 14 species and 65 cell types were examined. The examined exposure durations ranged from 5 min to 6 days for neuronal cells, with most publications examining the effects of electromagnetic fields (EMF) for 1, 2, 4 or 24 h. Based on these findings, 4 and 24 h exposure duration was chosen.

### 4.3 hOGG1-modified *in vitro* alkaline comet assay

The hOGG1-modified *in vitro* alkaline comet assay was performed according to the respective standard operating procedure (SOP) of ITEM. First, the microscope slides were coated with normal melting point agarose (NMA). Therefore, 40  $\mu$ l of NMA dissolved in PBS pre-warmed to 39 °C was pipetted onto a frosted slide and spread out using a plastic spatula. The slide was then dried on a 57 °C hot plate. After that, 100  $\mu$ l of the pre-warmed normal melting agarose was pipetted lengthwise on the slide and quickly covered with a coverslip to ensure even distribution of normal melting agarose. The coated slides were stored in a box with wet tissue paper in a refrigerator until further use.

For the positive controls, NHEK and NHEM were treated with 1  $\mu$ l/ml ethyl methanesulfonate (EMS) as direct clastogenic substance and 4 mM potassium bromate (KBrO<sub>3</sub>) as DNA oxidative stressor for 1 h. Since NHEM was observed to be not sensitive to KBrO<sub>3</sub>, we treated L-929 fibroblasts, originally derived from mouse connective tissue, with KBrO<sub>3</sub> as technical positive control for NHEM exposure.

The next steps were performed in a dark room with red light to avoid induction of unspecific, not substances dependent DNA strand breaks by UV irradiation. After the FR2 exposure, the cells were detached using the methods described in 4.1 without the centrifugation and resuspension

steps. 100 µl cell suspension were taken and pipetted into 10 ml CASYTon. Then the diluted cells were put into CASY® automatic cell counter with 150 µm measuring capillary to quantify the cell count. The viable cell counts were determined by the measuring cell size between 11.40 and 30.0 µm.

Each 900 µl of the cell suspension was transferred into 6 1.5 ml reaction tubes and centrifuged for 5 min at 106 x g. The coverslips of the pre-coated slides were removed, and the LMA-cell mixtures were pipetted onto the pre-coated slides. Afterwards, the slides were quickly covered using new coverslips and refrigerated for 10 minutes to harden the agarose. Then, the coverslips were removed to add 100 µl of LMA and covered the slide with a coverslip again. The slides were then refrigerated for another 10 minutes. Finally, the coverslip was removed, and the slides were put into lyse buffer overnight.

On the next day, the slides were then incubated twice with HEPES buffer at pH 8 for 5 min. Then, 3 slides from each exposure were incubated with only HEPES buffer or HEPES buffer with the addition of 0.2% hOOG1 enzyme for 15 min at 37 °C. The slides were placed into an ice cooled electrophoresis chamber and the electrophoresis buffer (4 °C) was poured into the chamber until the slide was covered and the power supply showed 24 V (voltage) as well as the amperage was between 300 mA and 320 mA. Thereafter, the slides were incubated in the electrophoresis chamber for 20 minutes. Subsequently, the electrophoresis was performed for 20 minutes. Afterwards, the slides were washed three times with Tris-HCl to neutralize the pH. Finally, the slide was stained with 80 µl of an ethidium bromide solution and stored in a box with wet tissue paper to prevent slide drying until evaluation.

Comets were quantified using the Comet Assay IV software from Perceptive Instruments Ltd. (now Instem), by counting of 150 nuclei per slide.

#### 4.4 Transcriptome analysis

The primary cells were seeded at a minimum of  $5 \cdot 10^5$  cells/ flasks prior to FR2 ensuring that enough RNA samples can be isolated for the microarray analyses. Due to the slow growth of the cells, we pooled the cells from more than 1 vial from the working batch to get enough cells, which was challenging due to limited quantity of available cells. Three experiments were performed on three different days, with three cell culture flasks for each condition exposed to 5G FR2 for 24 hours each day (n=9).

For cell harvesting, cells were washed twice with 2 ml pre-warmed PBS and 3 ml cold PBS were finally pipetted into the cell flasks for cell scraping. The resulting cell suspension was then transferred to a 15 ml centrifuge tube, and the cell culture flask was washed with another 3 ml of cold PBS and again transferred to the centrifuge tube. The final cell suspension was then centrifuged at 303 x g for 10 min and the supernatant removed. RNA was isolated and purified using the RNeasy (Plus) MiniKit (Qiagen, Hilden, Germany) and treated with DNase. In parallel

RNA isolation from an A549 cell pellet (250,000 cells) served as a kit control. RNA concentration (A260) and purity (A260/A280 ratio) was measured by spectrophotometry (NanoDrop™ 2000 Spectrophotometer, ThermoFisher Scientific, Waltham, United States of America). RNA integrity number (RIN) was evaluated using an Agilent 2100 Bioanalyzer® (Agilent Technologies, California, United States of America).

Transcriptome analyses were performed using the Affymetrix GeneChip™ Whole Transcript (WT) PLUS Reagent Kit and GeneChip™ human Clariom™ S Arrays (>20,000 well-annotated genes) according to the manufacturer's recommendation (Applied Biosystems, California, United States of America). A total RNA of 100 ng was used as a starting material for target preparation. Arrays were subsequently washed, stained, and scanned using the Affymetrix GeneChip™ Command Console Software (ThermoFisher Scientific) with “.cel” files as data output, which store the results of intensity calculations of pixel values based on the scanned pictures of the array.

The “.cel” files were then uploaded to Transcriptomics Analysis Console (TAC, Applied Biosystems, California, United States of America) to first assess the data quality. Here, TAC examined whether the target labeling and hybridization steps are performed correctly by calculating spike RNA and poly-A RNA signal intensities.

Differentially Expressed Genes (DEGs) were then analyzed using TAC by comparing the FR2- and sham-exposed cells with the filter of gene-level fold change (FC) < -2 or > 2, a *p*-value of 0.05, and a false discovery rate (FDR) of 0.05 determined by the eBayes Anova method. The data were then uploaded to Ingenuity Pathway Analysis (IPA, Qiagen) to identify possible affected pathways, functions and upstream regulators.

#### 4.5 DNA methylation

The cells were plated, exposed to 5G FR2 and harvested using the same protocol used for cell harvest for RNA isolation (see section 4.4). For the DNA methylation assay, three experiments were performed on three different days, with one cell culture flask for each condition exposed to 5G FR2 for 24 hours each day (n=3).

DNA was subsequently isolated using the NucleoSpin Tissue Kit (Macherey-Nagel). In parallel DNA isolation from an A549 cell pellet (250,000 cells) served as a kit control. DNA concentration (A260) and purity (A260/A280 ratio) was measured by spectrophotometry (NanoDrop™ 2000 Spectrophotometer, ThermoFisher Scientific).

Further processing was done in an external company, Hologic Diagenode (Seraing, Belgium), that also re-quantified the DNA samples using Qubit® dsDNA HS Assay Kit (ThermoFisher Scientific). A minimum of 250 ng DNA was used as starting material. The DNA was then processed using Illumina® Infinium® MethylationEPIC v2.0 kits, where the DNA underwent bisulfite conversion, amplification and hybridization to the array. The array was finally washed, stained and scanned

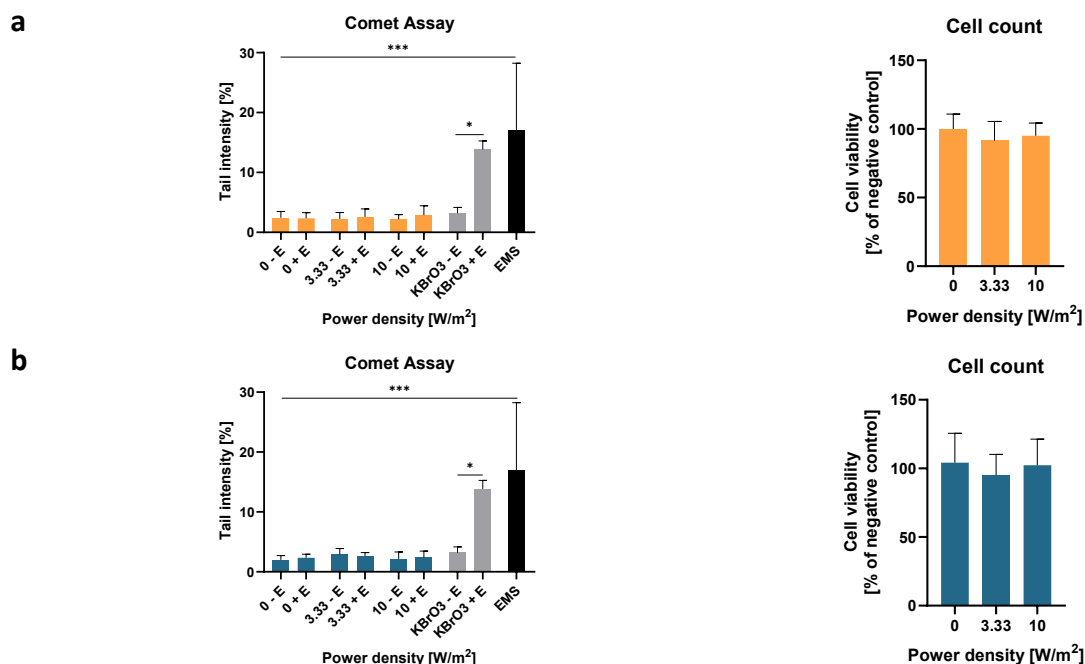
resulting in “.IDAT” files as data output, which contain the raw intensity data from the array, such as the mean, standard deviation and number of beads for each probe type on the array.

## 5 Results

### 5.1 hOGG1-modified *in vitro* alkaline comet assay

To investigate genotoxicity and oxidative DNA damage after exposure of the primary skin cells to 5G FR2, we performed hOGG1 enzyme-modified *in vitro* alkaline comet assay with parallel cytotoxicity test based on cell proliferation by cell counting to exclude unspecific genotoxic effects due to cell death.

After 4 h of exposure, 5G FR2 did not cause DNA damage when comparing the median tail intensities (TI) of exposure groups without hOGG1 treatment in all primary skin cell models. Furthermore, oxidative DNA lesions were also not detected in all exposure groups, when we compared the untreated and hOGG1-treated slides. No decrease in cell counts were detected in all exposure groups (see Figure 6). However, the positive control for oxidatively damaged DNA, i.e.,  $\text{KBrO}_3$ , did not work properly in NHEM, which was most likely due to the antioxidative effect of melanin (see Figure 6c, left) [26]. Thus, for the 24 h exposure to 5G FR2, we included another cell line as positive control.





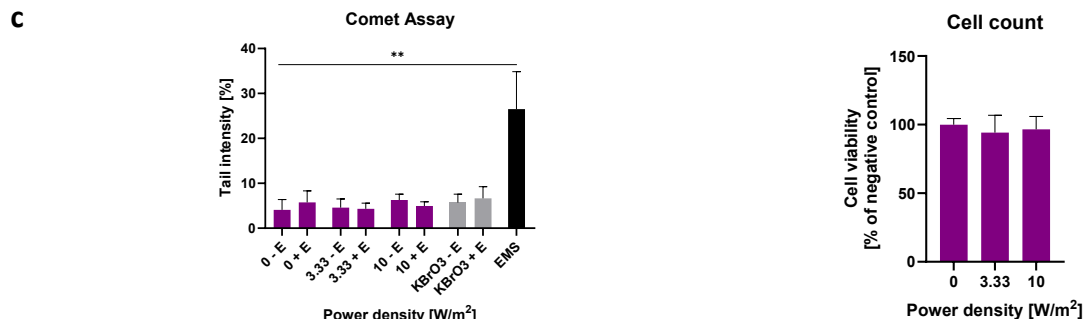
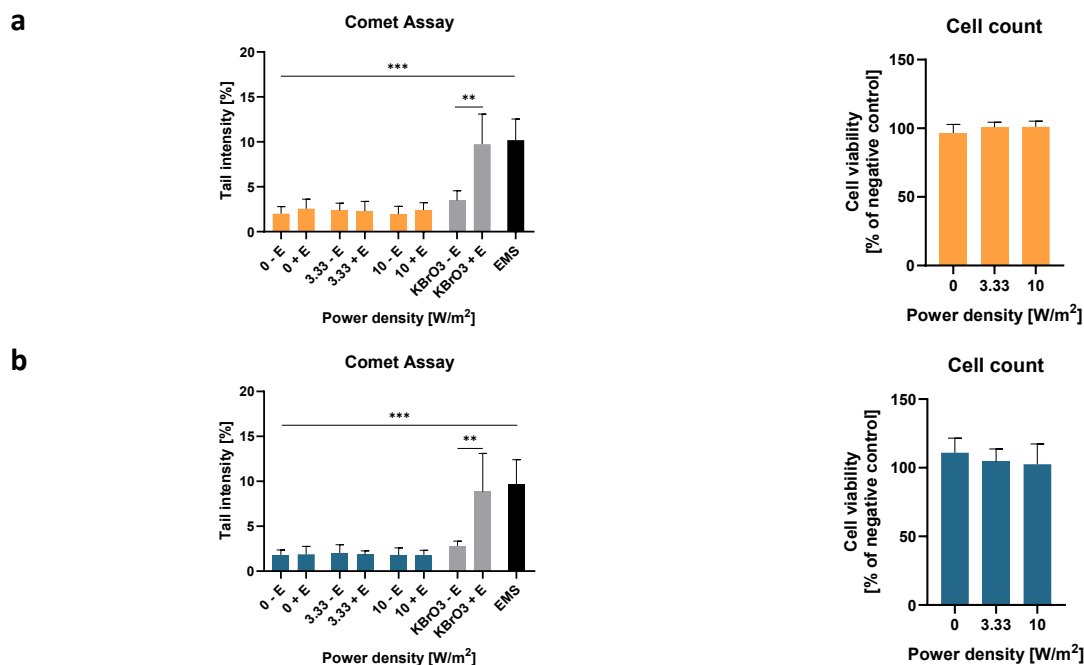


Figure 6: (Geno)toxicity of FR2 in NHEK-c. (a), NHEK-f.c. (b) and NHEM (c). Cells were pre-cultured for 24 h (NHEKs) or 72 h (NHEM), then exposed to 5G FR2 for 4 h. Data of the hOOG1-modified alkaline comet assay (tail intensity; left) and relative cell viability (based on cell counts; right) represent means  $\pm$  SD of three independent experiments with three replicates each. Comet assay mean data are derived from the median values of three biological replicates per experiment. Statistics was done using One-Way ANOVA with Dunnett's multiple comparisons test, as post hoc test, compared to sham-exposed slides. hOOG1-untreated were compared with hOOG1-treated slides using the paired *t*-test (tail intensity with hOOG1 > tail intensity without hOOG1 = oxidative DNA damage). For statistical comparison of EMS positive controls with respective negative controls, Student's *t*-test was performed, where \*  $p < 0.05$ , \*\*  $p < 0.01$ , \*\*\*  $p < 0.001$ .

In the NHEM experiments with 24 h of exposure, we included KBrO<sub>3</sub>-treated L-929 fibroblasts, originally derived from mouse connective tissue, as technical positive control for oxidatively damaged DNA. After 24 h of exposure, 5G FR2 also did not cause any DNA damage, i.e., DNA strand breaks or oxidative DNA lesions, or cytotoxic effects.



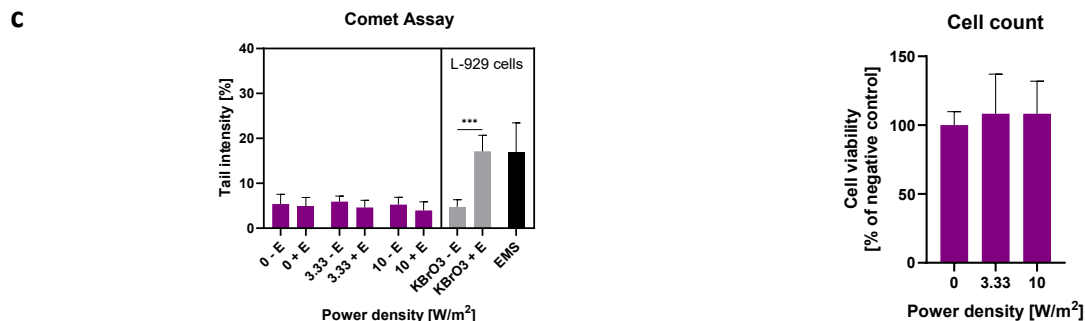


Figure 7: (Geno)toxicity of FR2 in NHEK-c. (a), NHEK-f.c. (b) and NHEM (c). Cells were pre-cultured for 24 h (NHEKs) or 72 h (NHEM), then exposed to 5G FR2 for 24 h. Data of the hOOG1-modified alkaline comet assay (tail intensity; left) and relative cell viability (based on cell counts; right) represent means  $\pm$  SD of three independent experiments with three replicates each. Comet assay mean data are derived from the median values of three biological replicates per experiment. Statistics was done using One-Way ANOVA with Dunnett's multiple comparisons test, as post hoc test, compared to sham-exposed slides. hOOG1-untreated were compared with hOOG1-treated slides using paired *t*-test (tail intensity with hOOG1 > tail intensity without hOOG1 = oxidative DNA damage). For statistical comparison of EMS positive controls with respective negative controls, Student's *t*-test was performed, where \*  $p < 0.05$ , \*\*  $p < 0.01$ , \*\*\*  $p < 0.001$ .

In conclusion, 5G FR2 exposure did not induce DNA strand breaks, oxidative DNA lesions or cytotoxicity after both 4 and 24 h, and modulation of DNA repair or antioxidant enzyme genes seemed unlikely to occur. To verify the possible antioxidant effects of melanin in NHEM, another experiment using hydrogen peroxide will be performed.

## 5.2 Transcriptomics

For task 8.5, transcriptomics analyses were performed to look for gene expression changes in the primary skin cell models after exposure to 5G FR2. Therefore, we used microarray technology from Affymetrix to screen a large set of known genes. As worst-case scenario, we also investigated the gene expression patterns of the melanoma cell lines MelHO and IPC-298.

After 5G FR2 exposure, subsequent cell harvest, RNA isolation and quantification, and microarray analysis, we confirmed whether the results files from the microarray passed the transcriptome analysis console (TAC) criteria in terms of quality control of microarray analysis and data. In this case, all data passed the quality control of TAC.

Principal component analysis (PCA) mapping for primary skin cells detected large transcriptome differences, as compared to the melanoma cell lines MelHO and IPC-298, used as worst-case scenario. As examples, Figure 8 depicted the PCA mappings between NHEK-f.c. and IPC-298, as well as NHEM and MelHO.

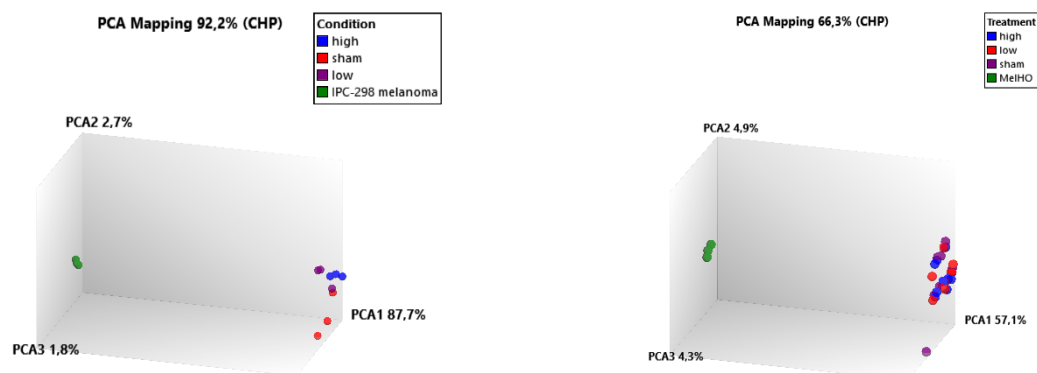
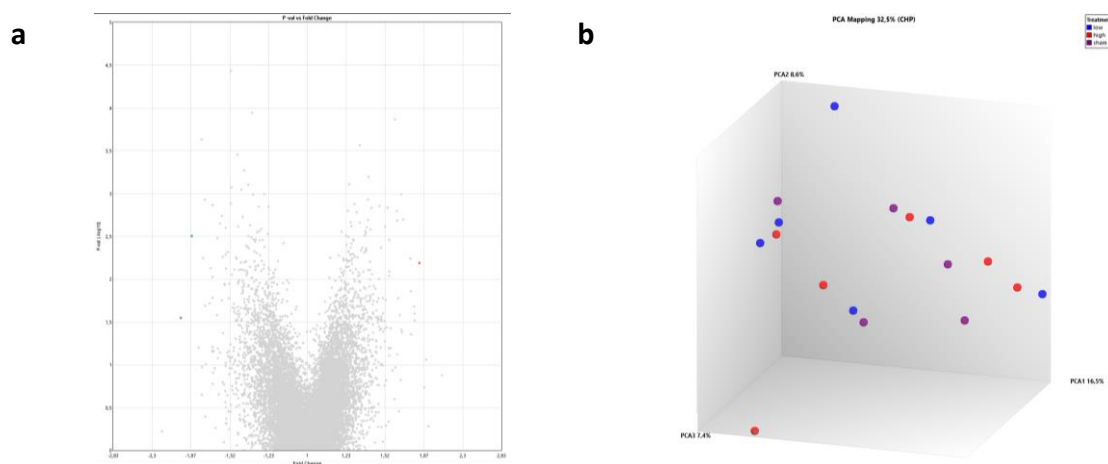


Figure 8: Principal component analysis (PCA) mapping of transcriptome between primary juvenile human epidermal keratinocytes (NHEK-f.c.) after exposure to fifth generation of mobile telephony frequency range 2 (5G FR2) at 27.5 GHz for 24 h and melanoma cell line IPC-298 (left), as well as between primary adult human epidermal melanocytes (NHEM) after exposure to 5G FR2 for 24 h and melanoma cell line MelHO (right).

When comparing all samples classified by conditions, there were no differentially expressed genes (DEGs) observed in NHEK-f.c. cells. In Figure 9A the respective volcano plots from comparison between low power density (low) vs sham exposure are depicted. The PCA, however, showed variability among the exposure groups (see Figure 9B). Therefore, comparisons between the conditions were performed within each batch. Using this setting, we observed that there were more DEGs in the low vs the sham exposure groups than in the high-power density (high) vs sham exposure groups in all three batches (see Figure 9C).



c

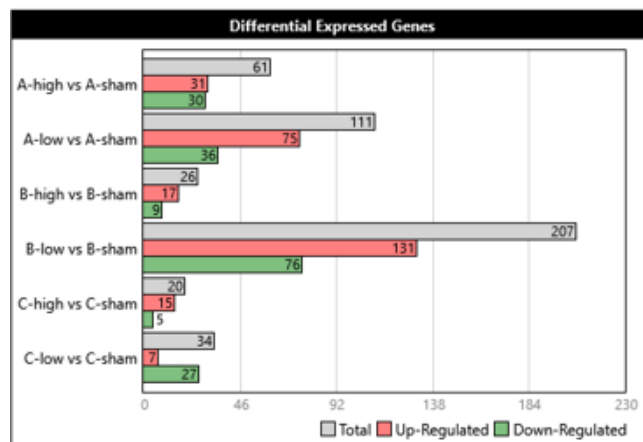


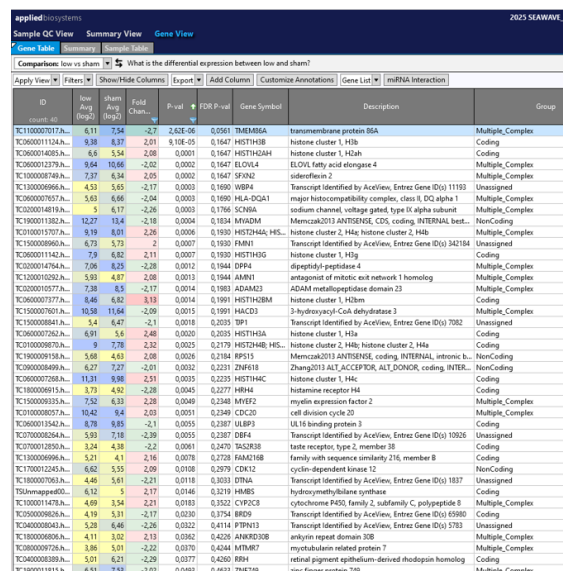
Figure 9: Transcriptomics results of primary juvenile human epidermal keratinocytes (NHEK-f.c.) after exposure to fifth generation of mobile telephony frequency range 2 (5G FR2) at 27.5 GHz with power density of 10 W/m<sup>2</sup> (high), 3.33 W/m<sup>2</sup> (low) and sham exposure for 24 h. a showed the principal component analysis (PCA) mapping of the exposure groups, b depicted the volcano plot differentially expressed genes (DEGs) from low vs sham exposure and c presented the DEGs using comparison between the conditions (low vs sham exposure and high vs sham exposure) within each group, where A, B and C represented the experiment repetition. The filter used were fold change of <-2 and >2, p-value of 0.05 and false discovery rate of 0.05.

Using these data, we also analyzed the possibly affected pathways using Ingenuity Pathway Analysis (IPA, Qiagen); considering the low responsiveness of the cells towards stress the fold change filter was reduced to <-1.5 and >1.5. With this approach we observed at last some pathway predicted to be activated or inhibited. The pathways, “mitochondrial dysfunction” and “extracellular matrix organization” were shown to be somehow affected/activated at low 5G FR2 exposure. On the other hand, “triacylglycerol biosynthesis”, “asparagine N-linked glycosylation” and “neutrophil degranulation” were predicted to be inhibited at low 5G FR2 exposure. Also, “renin-angiotensin signaling” was predicted to be inhibited after high 5G FR2 exposure.



Figure 10: An excerpt of Ingenuity Pathway Analysis (IPA, Qiagen) predicting affected pathways after exposure of primary juvenile human epidermal keratinocytes (NHEK-f.c.) to fifth generation of mobile telephony frequency range 2 (5G FR2) at 27.5 GHz with power density of 10 W/m<sup>2</sup> (high), 3.33 W/m<sup>2</sup> (low) and sham exposure for 24 h, where A and B represented the experiment repetition. The filter used were fold change of <-1.5 and >1.5, p-value of 0.05 and false discovery rate of 0.05.

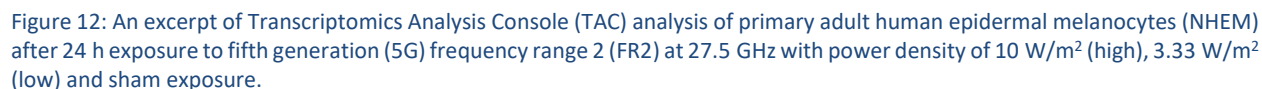
In agreement with the juvenile keratinocytes also in the NHEK-c., we observed that there might be more DEGs in low vs sham exposure groups. However, the false discovery rate (FDR) in all DEGs was higher than the threshold of 0.05. Thus, we concluded that there were virtually no effects to be observed in gene expression after exposure to 5G FR2.



ID	low vs sham	sham vs high	Fold Change	P-val	FDR P-val	Gene Symbol	Description	Group
TC100007017h	6.11	7.54	-2.7	2.6E-06	0.0561	TMEM65A	transmembrane protein 65A	Multiple_Complex
TC0600011124h	9.38	8.97	2.01	5.10E-05	0.1647	HISTH3B	histone cluster 3, H3b	Coding
TC0600014025h	6.8	5.54	2.08	0.0001	0.1647	HISTH4A	histone cluster 4, H4a	Coding
TC0600012379h	9.64	10.66	-2.02	0.0002	0.1647	ELOVL4	ELOVL4 fatty acid elongase 4	Multiple_Complex
TC100000748h	7.37	6.34	2.05	0.0002	0.1647	SFOK2	sideroflexin 2	Multiple_Complex
TC100000696h	4.53	5.65	-2.17	0.0003	0.1689	WBK4	Transcript identified by AcVies, Entrez Gene ID(s) 11193	Unassigned
TC0600010757h	5.63	6.66	-2.04	0.0003	0.1689	HLA-DQA1	major histocompatibility complex, class II, DQ alpha 1	Multiple_Complex
TC0200014818h	5	6.17	-2.26	0.0003	0.1766	SCN8A	sodium channel, voltage gated, type IX alpha subunit	Multiple_Complex
TC1900011382h	12.27	13.4	-2.18	0.0004	0.1834	MVAD4	Mernca2013 ANTISENSE, CDS, coding, INTERNAL, best...	NonCoding
TC1900011577h	9.19	8.01	2.26	0.0004	0.1939	HISTH2AA.HS	histone cluster 2, H4a, histone cluster 2, H4a	Multiple_Complex
TC150000960h	6.73	5.73	2	0.0007	0.1939	FRN1	Transcript identified by AcVies, Entrez Gene ID(s) 342184	Unassigned
TC0600011142h	7.9	6.82	2.11	0.0007	0.1939	HISTH3G	histone cluster 3, H3g	Coding
TC020001476h	7.08	6.25	2.28	0.0012	0.1944	EPH4	ephrin type 4, protein tyrosine kinase	Multiple_Complex
TC1200012052h	5.93	4.87	2.08	0.0013	0.1944	AMRN1	antagonist of mitotic exit network 1 homolog	Multiple_Complex
TC0200010577h	7.38	6.5	2.17	0.0014	0.1983	ADAM23	ADAM metalloproteinase domain 23	Multiple_Complex
TC0600010777h	8.46	6.82	2.13	0.0014	0.1983	HISTH3BM	histone cluster 3, H3bm	Coding
TC1500010769h	10.58	11.64	-2.06	0.0015	0.1991	HACD3	3-hydroxyacyl-CoA dehydrogenase 3	Multiple_Complex
TC1500008841h	5.4	6.47	-2.1	0.0018	0.2035	TP1	Transcript identified by AcVies, Entrez Gene ID(s) 7082	Unassigned
TC0600010762h	6.91	5.6	2.48	0.0020	0.2035	HISTH3A	histone cluster 3, H3a	Coding
TC1000006970h	9	7.28	2.32	0.0023	0.2175	HISTH4B.HS	histone cluster 2, H4b, histone cluster 2, H4b	Coding
TC1900009158h	5.68	4.63	2.08	0.0028	0.2184	RPS15	Mernca2013 ANTISENSE, coding, INTERNAL, intronic b...	NonCoding
TC0900004049h	6.27	7.27	-2.01	0.0032	0.2231	ZNF618	Zhang2013 ALT, ACCEPTOR, ALT_DONOR, coding, INTER...	NonCoding
TC0600010768h	11.31	9.98	2.51	0.0035	0.2235	HISTH4C	histone cluster 4, H4c	Coding
TC1800006915h	3.73	4.92	-2.28	0.0045	0.2277	HNR4	histone receptor 4d	Coding
TC1500009335h	7.52	6.33	2.28	0.0048	0.2348	MVIF2	myelin expression factor 2	Multiple_Complex
TC1000008057h	10.42	9.4	2.03	0.0051	0.2349	CDC20	cell division cycle 20	Multiple_Complex
TC0600011342h	8.78	6.95	2.1	0.0055	0.2387	ULBP3	LE18 binding protein 3	Coding
TC0700008264h	5.93	7.18	-2.39	0.0055	0.2387	DBF4	Transcript identified by AcVies, Entrez Gene ID(s) 10926	Unassigned
TC0700012850h	1.34	4.38	-2.2	0.0061	0.2470	TAS2R38	taste receptor, type 2, member 38	Coding
TC1300006995h	5.21	4.1	2.16	0.0078	0.2728	FAM421B	family with sequence similarity 276, member B	Coding
TC1700012454h	6.62	5.55	2.09	0.0108	0.2978	CDK12	cyclin-dependent kinase 12	NonCoding
TC1800007063h	4.46	5.61	-2.21	0.0118	0.3033	DTNA	Transcript identified by AcVies, Entrez Gene ID(s) 1837	Unassigned
TS9unmapped0	6.12	5	2.17	0.0146	0.3219	HA85	hydroxymethylglutathione synthase	Coding
TC100001476h	4.69	3.54	2.21	0.0183	0.3523	CYP2C8	cytochrome P450 family 2, subfamily C, polypeptide 8	Multiple_Complex
TC0500008826h	4.19	5.31	-2.17	0.0230	0.3754	BRD9	Transcript identified by AcVies, Entrez Gene ID(s) 65980	Coding
TC0400008042h	5.28	6.46	-2.26	0.0322	0.4114	PTPN13	Transcript identified by AcVies, Entrez Gene ID(s) 5783	Unassigned
TC100000695h	4.11	3.02	2.13	0.0342	0.4239	MYRM20B	myrin repeat domain 20B	Multiple_Complex
TC0800009726h	3.86	5.01	-2.22	0.0370	0.4384	MTM87	myotubularin related protein 7	Multiple_Complex
TC0400008389h	5.01	6.21	-2.29	0.0377	0.4590	R9H4	retinal pigment epithelium-derived rhodopsin homolog	Coding
TC1900011815h	6.51	7.53	-2.02	0.0483	0.4833	ZNF749	zinc finger protein 749	Multiple_Complex

Figure 11: An excerpt of Transcriptomics Analysis Console (TAC) analysis of primary adult human epidermal keratinocytes (NHEK-f.c.) after 24 h exposure to fifth generation (5G) frequency range 2 (FR2) at 27.5 GHz with power density of 10 W/m<sup>2</sup> (high), 3.33 W/m<sup>2</sup> (low) and sham exposure.

In NHEM, we also observed more DEGs in the low vs sham exposure groups than in the high vs sham exposure groups. Similar to NHEK-c., however, the FDR was higher than the threshold of 0.05. We also concluded that there were no effects on gene expression of 5G FR2 exposure in NHEM.



**Gene Set 1: 1000 Genes**  
 Control: 1000 Genes  
 Deletion: 1000 Genes  
 Duplication: 1000 Genes

**Gene Set 2: 1000 Genes**  
 Control: 1000 Genes  
 Deletion: 1000 Genes  
 Duplication: 1000 Genes

**Gene Set 3: 1000 Genes**  
 Control: 1000 Genes  
 Deletion: 1000 Genes  
 Duplication: 1000 Genes

In conclusion, we observed no effects of 5G FR2 exposure after 24 h on gene expression regulation in all tested primary skin cell models. In mice modulated genes after 5G FR2 exposure, there was no changes to be observed in NHEK-f.c., NHEK-c. and NHEM.

### 5.3 DNA methylation assay

For task 8.4, we also determined the effects of FR2 exposure on the epigenome of the NHEK and NHEM, as most important skin cell types. Additionally, we also analyzed the epigenome of MelHO and IPC-298 cell line as worst-case references. The isolated DNA was then quantified using NanoDrop™ 2000 spectrophotometer prior delivering the DNA samples to Diagenode Hologic, Seraing, Belgium for further analysis.

However, there are scientific discussion about the NanoDrop™ DNA quantification system, due to possible inaccurate results and, thus, the DNA samples were re-evaluated by using Qubit® dsDNA HS Assay kit. The overview of the results from both quantification methods is depicted in Table 2 showing some noteworthy deviations in both methods even though it was assumed to be a simple approach.

Table 2: Overview of DNA quantification using NanoDrop™ 2000 Spectrophotometer and Qubit® dsDNA HS Assay Kit.

Cell type	Sample name	Treatment	Repetition	Cell count [· 10 <sup>5</sup> cells]	DNA concentration using NanoDrop [ng/μl]	DNA concentration using Qubit [ng/μl]
NHEK-c.	NHEK-c-1-1	Chamber 1	1	6.810	20.24	13.4
	NHEK-c-1-2	Chamber 2		7.670	15.83	11.8
	NHEK-c-1-3	Chamber 3		6.738	20.65	11.3
	NHEK-c-2-1	Chamber 1	2	4.527	19.92	10.3
	NHEK-c-2-2	Chamber 2		5.192	18.46	7.04
	NHEK-c-2-3	Chamber 3		5.039	14.18	5.02*
	NHEK-c-3-1	Chamber 1	3	4.534	21.53	9.8
	NHEK-c-3-2	Chamber 2		4.554	22.14	9.52
	NHEK-c-3-3	Chamber 3		4.725	22.70	9.92
NHEK-f.c.	NHEK-fc-1-1	Chamber 1	1	5.164	25.55	4.9*
	NHEK-fc-1-2	Chamber 2		5.684	26.33	6.52
	NHEK-fc-1-3	Chamber 3		6.185	36.86	6.44
	NHEK-fc-2-1	Chamber 1	2	7.312	25.76	6.42
	NHEK-fc-2-2	Chamber 2		7.498	36.29	14.1
	NHEK-fc-2-3	Chamber 3		7.488	42.94	5.22*
	NHEK-fc-3-1	Chamber 1	3	7.870	20.52	14.1
	NHEK-fc-3-2	Chamber 2		7.738	20.73	7.22
	NHEK-fc-3-3	Chamber 3		7.964	14.12	10.2
NHEM	NHEM-1-1	Chamber 1	1	4.583	64.46	9.16
	NHEM-1-2	Chamber 2		4.976	69.75	9.16
	NHEM-1-3	Chamber 3		4.675	70.87	17.6
	NHEM-2-1	Chamber 1	2	3.286	51.36	5.26*



	NHEM-2-2	Chamber 2		4.515	47.34	6.54
	NHEM-2-3	Chamber 3		4.250	101.74	6.56
	NHEM-3-1	Chamber 1		3.415	16.13	5.48
	NHEM-3-2	Chamber 2	3	2.988	7.20	3.48*
	NHEM-3-3	Chamber 3		3.344	12.86	5.54
MelHO	MelHO-1	untreated		~5	49.86	22.8
	MelHO-2	untreated	-	~5	53.49	21.3
	MelHO-3	untreated		~5	40.33	26.6
IPC-298	IPC-298-1	untreated		~5	94.42	35
	IPC-298-2	untreated	-	~5	69.03	20.6

\* Below recommended DNA concentration for Illumina® array

Generally, the quantification using Qubit was lower in comparison to quantification via NanoDrop™. However, the amount of DNA isolated for the following microarray analysis was sufficient except for 5 samples, which needed to be further concentrated in order to reach recommended DNA concentration for the Illumina® Infinium® MethylationEPIC v2.0 array analysis. The analysis is still ongoing as of 25.06.2025 and estimated to be finished on 15.07.2025.

## 6 Conclusions

After carefully selected the primary human-derived skin cells based on tissue origin, sex, age and skin pigmentation, we examined the genotoxicity, oxidative DNA damage, transcriptomics and epigenomics changes of the primary skin cells after exposure to 5G FR2.

In the comet assay, 5G FR2 exposure to the primary skin cells did not induce any DNA strand breaks and oxidative DNA lesions. Furthermore, no cytotoxic effects were observed after 4 and 24 h exposure.

Primary adult human epidermal keratinocytes and melanocytes (NHEK-c. and NHEM, respectively) 5G FR2 showed no effects on gene expression i.e., changes in DEG numbers. Therefore, no pathway analyses were performed.

However, primary juvenile human epidermal keratinocytes (NHEK-f.c.) presented some DEGs after 5G FR2 exposure within the false discovery rate (FDR), when comparing the conditions within each exposure group. The pathway analyses predicted that some pathways were activated and inhibited mostly in low 5G FR2 exposure.

After cell harvesting and DNA isolation of the primary skin cells, further processing is done in an external company, Hologic Diagenode, Belgium. As of 25.06.2025 the processing is still ongoing. The DNA methylation assay is estimated to be finished on 15.07.2025.

## 7 References

1. Belli M, Tabocchini MA. Ionizing Radiation-Induced Epigenetic Modifications and Their Relevance to Radiation Protection. *International Journal of Molecular Sciences*. 2020;21(17):5993.
2. Manser M, Sater MRA, Schmid CD, Noreen F, Murbach M, Kuster N, et al. ELF-MF exposure affects the robustness of epigenetic programming during granulopoiesis. *Scientific Reports*. 2017;7(1):43345.
3. Reamon-Buettner SM, Heimisch A, Lewin G, Dasenbrock C, Halter R, editors. Single-promoter analysis of CpG and non-CpG methylation patterns in spleen of mice exposed to extremely low frequency magnetic field (ELF-MF). *Deutsche Gesellschaft für Experimentelle und Klinische Pharmakologie und Toxikologie eV Abstracts of the 81th Annual Meeting*; 2015; Kiel, Germany: Naunyn-Schmiedeberg's Archives of Pharmacology
4. Ryu B, Kim DS, DeLuca AM, Alani RM. Comprehensive Expression Profiling of Tumor Cell Lines Identifies Molecular Signatures of Melanoma Progression. *PLOS ONE*. 2007;2(7):e594.
5. Jin S-G, Xiong W, Wu X, Yang L, Pfeifer GP. The DNA methylation landscape of human melanoma. *Genomics*. 2015;106(6):322-30.
6. Joushomme A, Orlicchio R, Patrignoni L, Canovi A, Chappe YL, Poullietier De Gannes F, et al. Effects of 5G-modulated 3.5 GHz radiofrequency field exposures on HSF1, RAS, ERK, and PML activation in live fibroblasts and keratinocytes cells. *Sci Rep*. 2023;13(1):8305.
7. Kim K, Lee YS, Kim N, Choi HD, Kang DJ, Kim HR, et al. Effects of Electromagnetic Waves with LTE and 5G Bandwidth on the Skin Pigmentation In Vitro. *Int J Mol Sci*. 2020;22(1):E170.
8. Kim K, Lee YS, Kim N, Choi HD, Lim KM. 5G Electromagnetic Radiation Attenuates Skin Melanogenesis In Vitro by Suppressing ROS Generation. *Antioxidants (Basel)*. 2022;11(8):1449.
9. Soubere Mahamoud Y, Aite M, Martin C, Zhadobov M, Sauleau R, Le Drean Y, et al. Additive Effects of Millimeter Waves and 2-Deoxyglucose Co-Exposure on the Human Keratinocyte Transcriptome. *PLoS One*. 2016;11(8):e0160810.
10. Jyoti J, Gronau I, Cakir E, Hütt M-T, Lerchl A, Meyer V. 5G-exposed human skin cells do not respond with altered gene expression and methylation profiles. *PNAS Nexus*. 2025;4(5):pgaf127.
11. Bertolotto C. Melanoma: from melanocyte to genetic alterations and clinical options. *Scientifica (Cairo)*. 2013;2013:635203.
12. Nadalutti CA, Wilson SH. Using Human Primary Foreskin Fibroblasts to Study Cellular Damage and Mitochondrial Dysfunction. *Curr Protoc Toxicol*. 2020;86(1):e99.
13. Martincorena I, Roshan A, Gerstung M, Ellis P, Van Loo P, McLaren S, et al. Tumor evolution. High burden and pervasive positive selection of somatic mutations in normal human skin. *Science*. 2015;348(6237):880-6.
14. Tai C, Xie Z, Li Y, Feng Y, Xie Y, Yang H, et al. Human skin dermis-derived fibroblasts are a kind of functional mesenchymal stromal cells: judgements from surface markers, biological characteristics, to therapeutic efficacy. *Cell & bioscience*. 2022;12(1):105.
15. Visscher MO, Hu P, Carr AN, Bascom CC, Isfort RJ, Creswell K, et al. Newborn infant skin gene expression: Remarkable differences versus adults. *PLoS One*. 2021;16(10):e0258554.

16. DSMZ. Mel-HO online: DSMZ-German Collection of Microorganisms and Cell Cultures GmbH; n.d. [Available from: <https://www.dsmz.de/collection/catalogue/details/culture/ACC-62>.
17. DSMZ. IPC-298: DSMZ-German Collection of Microorganisms and Cell Cultures GmbH; [Available from: <https://www.dsmz.de/collection/catalogue/details/culture/ACC-251>.
18. Davies H, Bignell GR, Cox C, Stephens P, Edkins S, Clegg S, et al. Mutations of the BRAF gene in human cancer. *Nature*. 2002;417(6892):949-54.
19. Moller P, Azqueta A, Boutet-Robinet E, Koppen G, Bonassi S, Milic M, et al. Minimum Information for Reporting on the Comet Assay (MIRCA): recommendations for describing comet assay procedures and results. *Nat Protoc*. 2020;15(12):3817-26.
20. Malone JH, Oliver B. Microarrays, deep sequencing and the true measure of the transcriptome. *BMC Biology*. 2011;9(1):34.
21. Staal FJ, van der Burg M, Wessels LF, Barendregt BH, Baert MR, van den Burg CM, et al. DNA microarrays for comparison of gene expression profiles between diagnosis and relapse in precursor-B acute lymphoblastic leukemia: choice of technique and purification influence the identification of potential diagnostic markers. *Leukemia*. 2003;17(7):1324-32.
22. Baylin SB, Jones PA. A decade of exploring the cancer epigenome — biological and translational implications. *Nature Reviews Cancer*. 2011;11(10):726-34.
23. Lakshminarasimhan R, Liang G. The Role of DNA Methylation in Cancer. *Adv Exp Med Biol*. 2016;945:151-72.
24. Sandoval J, Esteller M. Cancer epigenomics: beyond genomics. *Current Opinion in Genetics & Development*. 2012;22(1):50-5.
25. PROPRIETARY I. Infinium HD Methylation Assay Protocol Guide (15019519). In: Illumina, editor. [https://emeasupportillumina.com/content/dam/illumina-support/documents/documentation/chemistry\\_documentation/infinium\\_assays/infinium\\_hd\\_methylation/infinium-hd-methylation-guide-15019519-01pdf](https://emeasupportillumina.com/content/dam/illumina-support/documents/documentation/chemistry_documentation/infinium_assays/infinium_hd_methylation/infinium-hd-methylation-guide-15019519-01pdf). online2015.
26. Kowichi J, Walter CQ, Thomas BF, George S. Some Aspects Of Melanin Biology: 1950–1975. *Journal of Investigative Dermatology*. 1976;67(1):72-89.